

# Controlled Gelation of Poly(3-alkylthiophene)s in Bulk and Thin Films Environments using Low Volatility Solvent/Poor-Solvent Mixtures

*Gregory M. Newbloom<sup>‡</sup>, Pablo de la Iglesia<sup>‡</sup> and Lilo D. Pozzo\**

Department of Chemical Engineering, University of Washington, Box 351750, Seattle, Washington, 98195-1750, United States

\* Email: [dpozzo@u.washington.edu](mailto:dpozzo@u.washington.edu). <sup>‡</sup> These authors contributed equally to this work.

## **SUPPORTING INFO:**

### **1.1 P3HT Organogel Rheology Kinetics**

Conjugated polymer self-assembly is both a kinetically and thermodynamically driven process. The self-assembly kinetics can be tuned through changes in solvent ratio and concentration as well as through changes in cooling rate. Figure S1 shows the rheology of a P3HT organogels at different cooling rates. As expected, faster cooling rates lead lower gelation temperatures and slower cooling rates lead to higher gelation temperatures.

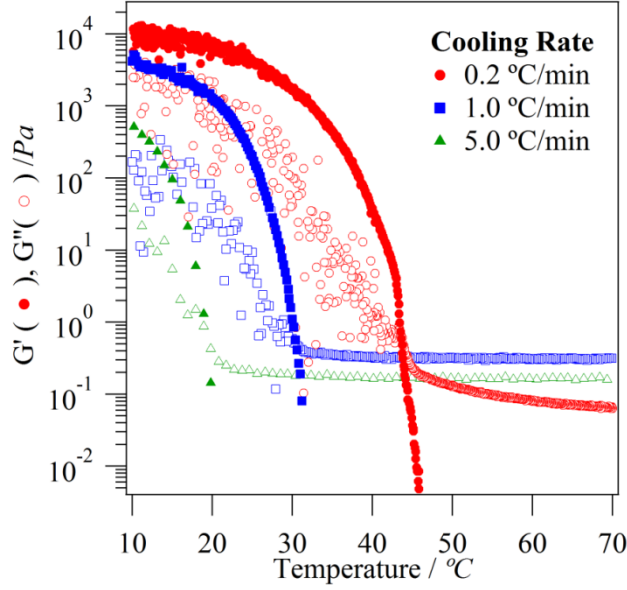


**Figure S1.** Rheology of 30 mg/mL High  $M_w$  P3HT in 43.9 wt% dodecane/ 56.1 wt% DCB measured during a cooling ramp from 80 °C to 10 °C.

## 1.2 SANS Model Fitting

The shape of the semi-crystalline P3AT fibers is represented by the parallelepiped form factor ( $P_{PP}(q)$ ):

$$P_{PP}(q, a, b, c) = \frac{2}{\pi} \int_0^{\pi/2} \int_0^{\pi/2} \left[ \left( \frac{\sin(qa \sin \alpha \cos \beta)}{qa \sin \alpha \cos \beta} \right) \left( \frac{\sin(qb \sin \alpha \cos \beta)}{qb \sin \alpha \cos \beta} \right) \left( \frac{\sin(qc \cos \alpha)}{qc \cos \alpha} \right) \right]^2 \sin(\alpha) d\alpha d\beta \quad (\text{S1})$$

where  $a$ ,  $b$  and  $c$  are the fiber thickness, width and length respectively.<sup>1</sup> The length of the fiber ( $c$ ) is expected to be significantly larger than the  $q$ -range probed in these experiments and has been previously shown to have an inconsequential effect on fitting.<sup>2</sup>

Dissolved P3AT chains are represented by a form factor for polymers with excluded volume effects ( $P_{ExV}(q)$ ):

$$P_{ExV}(q, n, a, \nu) = 2 \int_0^1 dx (1-x) \exp \left[ -\frac{q^2 a^2}{6} n^{2\nu} x^{2\nu} \right] \quad (\text{S2})$$

where  $n$  is the number of “Kuhn” segments,  $a$  is the Kuhn length and  $\nu$  is related to the conformation of the polymer chain.<sup>3</sup> For rod-like polymer chains  $\nu = 1$ , for Gaussian coils  $\nu = 0.5$  and for fully collapsed chains  $\nu = 0.33$ . These fitting parameters can be utilized to determine the radius of gyration ( $R_g$ ) using the following equation:

$$R_g^2 = \frac{a^2 n^{2\nu}}{(2\nu + 1)(2\nu + 2)} \quad (\text{S3})$$

Previous work has demonstrated that dissolved polymer chains exist at all stages of self-assembly, even in fully formed gels, and that the polymer conformation can be held constant to reduce the number of fitting parameters in the model.<sup>4, 5</sup> Dissolved P3AT conformations were determined from SANS profiles at time zero and are listed in Table S1. The results of the fits are in agreement with expectations based on the polymer properties (Main Text, Table 1). The radius of gyration scales with the length of the polymer chain and the spatial distribution of the polymer chain ( $\nu$ ) scales with the alkyl chain length. Schweizer predicted that increasing entropy from longer alkyl chains would result in increased backbone torsion and therefore less rigid conjugated polymer chains which is also in agreement with our findings.<sup>6</sup>

**Table S1.** The conformation of dissolved polymers at 30 °C as determined from SANS for 30 mg/mL high  $M_w$  P3HT in 43.9% dodecane/56.1% DCB, 30 mg/mL P3OT in 71.3% dodecane/28.7% DCB and 30 mg/mL P3DDT in 84.7% dodecane/15.3% DCB.  $R_g$  is the radius of gyration and  $\nu$  is related to the spatial distribution of the chain.

	$R_g$ (Å)	$\nu$
<b>High <math>M_w</math> P3HT</b>	54	0.78
<b>P3OT</b>	70	0.66
<b>P3DDT</b>	49	0.56

It is now well established that aromatic solvent molecules can also get trapped within fiber structures during self-assembly.<sup>2, 4, 5, 7-10</sup> The scattering length density (SLD) of P3AT fibers was determined by doing a contrast variation experiment. Figure S2 shows the SANS contrast variation experiment of P3AT organogels self-assembled in different dodecane/1,2-dichlorobenzene solvent mixtures where d4-1,2-dichlorobenzene was utilized while the ratio of deuterated/hydrogenated dodecane was varied before self-assembly. The SLD of each solvent mixture was determined from predicted densities and the molecular composition. The square-root intensity ( $I^{1/2}$ ) at a  $q$ -value ( $0.0031 \text{ \AA}^{-1}$ ) is plotted against the SLD and fit to find the zero-contrast point, which is equivalent to the SLD of the organogel.<sup>11</sup> The SLD of high  $M_w$  P3HT gels in different solvent mixtures can also be seen in Figure S2 and show little difference in the zero-contrast point.

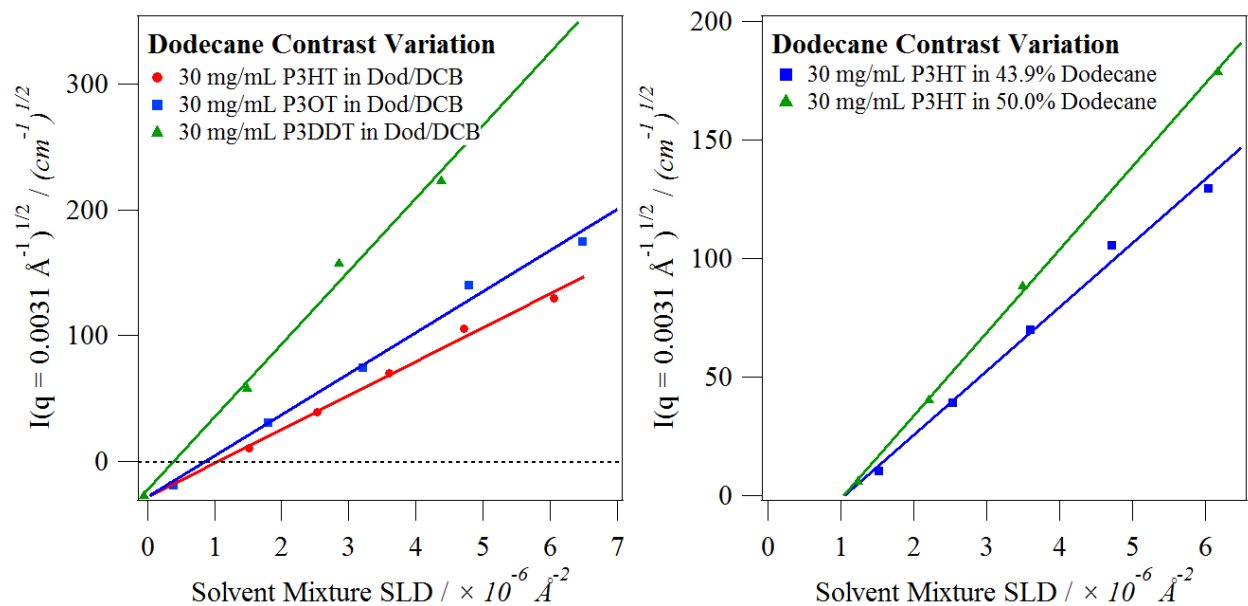


**Figure S2.** Square-root SANS intensity plotted against the scattering length density of a d26-dodecane/d4-1,2-dichlorobenzene solvent mixture for a 30 mg/mL high  $M_w$  P3HT gel in 43.9

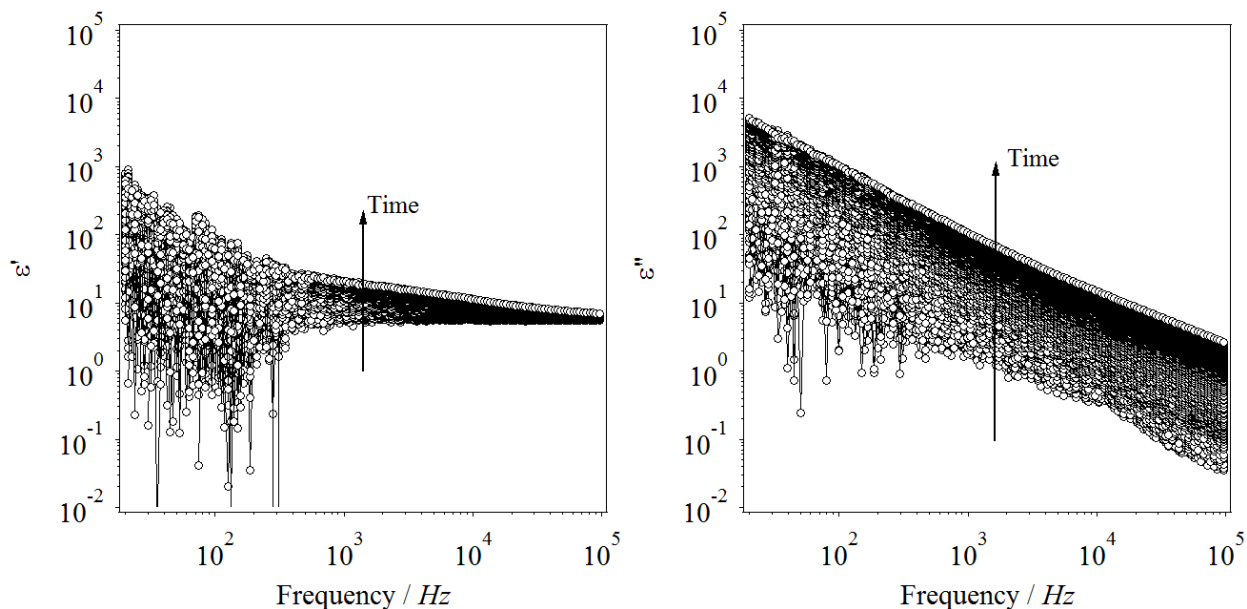
wt% dodecane/56.1 wt% DCB, 30 mg/mL P3OT gel in 71.3 wt% dodecane/28.7 wt% DCB and 30 mg/mL P3DDT gel in 84.7 wt% dodecane/15.3 wt% DCB (left) and for a 30 mg/mL high  $M_w$  P3HT gel in two solvent mixtures: 50.0 wt% dodecane/50.0 wt% DCB and 43.9 wt% dodecane/56.1 wt% DCB (right). All measurements were taken at 20 °C.

The measured SLD values for solvated P3HT, P3OT and P3DDT fibers were  $1.1 \times 10^{-6} \text{ \AA}^{-2}$ ,  $0.9 \times 10^{-6} \text{ \AA}^{-2}$  and  $0.4 \times 10^{-6} \text{ \AA}^{-2}$ , respectively. The SLD values correspond to fibers that contain ~14 wt% dichlorobenzene (High  $M_w$  P3HT and P3OT) or 5 wt% (P3DDT). Furthermore, there is no correlation between fiber SLD and solvent ratio, suggesting that solvent incorporation is limited by steric packing interactions as proposed by Zuo and coworkers.<sup>10</sup> Figure S2 also shows similar zero contrast points for P3HT in different dodecane/DCB ratios. This suggests that the amount of DCB in the fibers is identical, even though the solvent ratios differ. The SLD of fully dissolved P3HT, P3OT and P3DDT were calculated from their density and molecular composition to be  $0.7 \times 10^{-6} \text{ \AA}^{-2}$ ,  $0.5 \times 10^{-6} \text{ \AA}^{-2}$  and  $0.3 \times 10^{-6} \text{ \AA}^{-2}$ , which is similar to what others have measured.<sup>12, 13</sup>

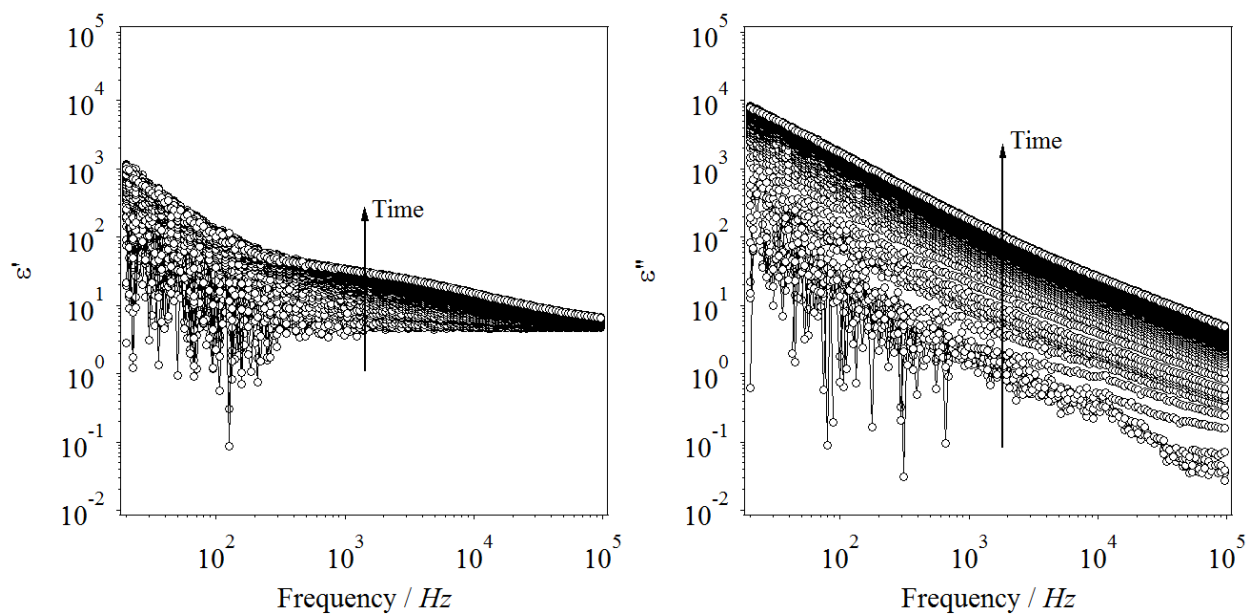
### 1.3 Dielectric Spectroscopy of P3AT Organogels

Figure S3-S6 shows the frequency-dependent dielectric spectrum (20 Hz to 200 kHz) taken as a function time during isothermal self-assembly for Low  $M_w$  and High  $M_w$  P3HT, P3OT and P3DDT organogels. Frequency sweeps were taken at 1 minute intervals. The dielectric spectrums, except that of P3DDT, show an increase in both  $\epsilon'$  and  $\epsilon''$  as a function of time. Figures S3-S5 show changes in the slope of  $\epsilon'$  around a frequency of 100 Hz and 20 kHz that arise during the self-assembly process. It may be possible to attribute these relaxations to structural features within the gel, but additional experiments are required to accomplish this.

Figure S7 shows the characteristic Nyquist plots for High  $M_w$  P3HT under the same self-assembly conditions with sweeps taken at 15 minute intervals. Figure S8 shows the frequency dependent conductivity profiles during the self-assembly of a P3OT organogel. This figure indicates that the magnitude of the conductivity response is frequency dependent. However, the conductivity kinetics are nearly identical for varying frequencies.



**Figure S3.** The real (left) and imaginary (right) dielectric constants as function of frequency taken during the self-assembly of a 30 mg/mL Low  $M_w$  P3HT gel in 27.5% dodecane/72.5% DCB at isothermal conditions (20 °C).



**Figure S4.** The real (left) and imaginary (right) dielectric constants as function of frequency taken during the self-assembly of a 30 mg/mL High  $M_w$  P3HT gel in 43.9% dodecane/56.1% DCB at isothermal conditions (30 °C).

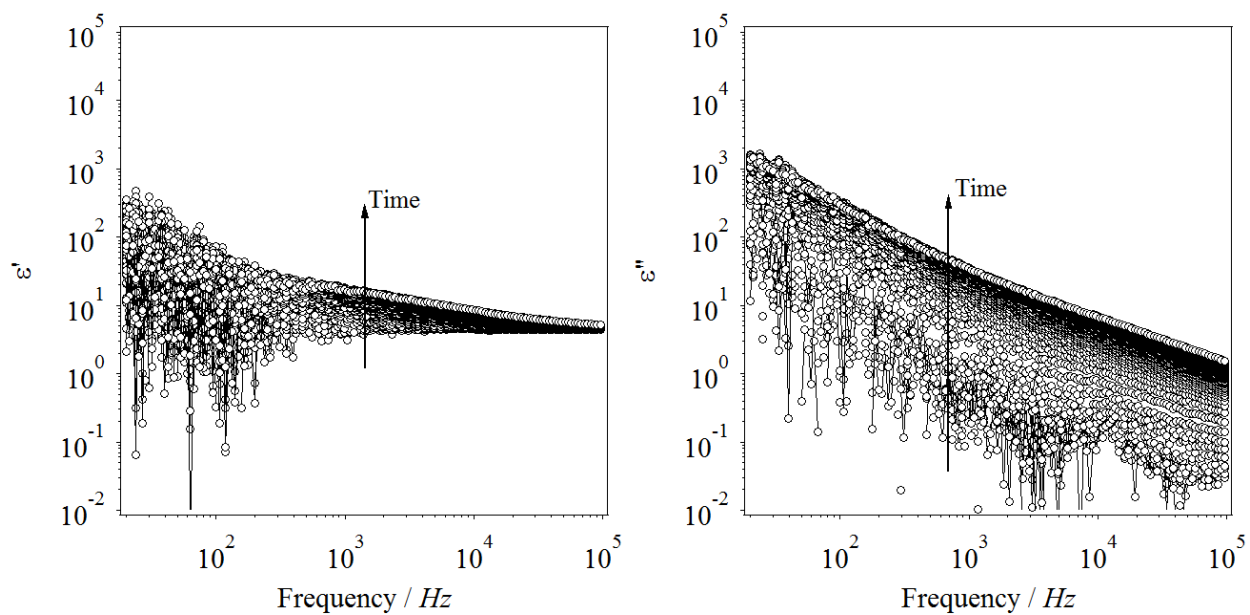


**Figure S5.** The real (left) and imaginary (right) dielectric constants as function of frequency taken during the self-assembly of a 30 mg/mL P3OT gel in 71.3% dodecane/28.7% DCB at isothermal conditions (30 °C).



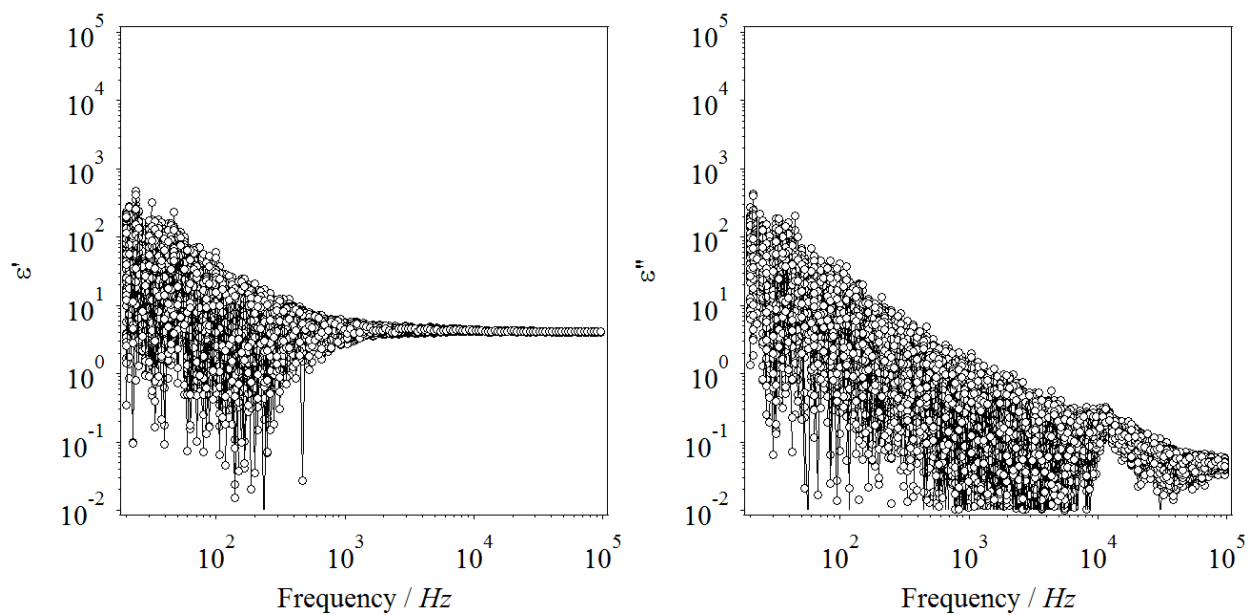


**Figure S6.** The real (left) and imaginary (right) dielectric constants as function of frequency taken during the self-assembly of a 30 mg/mL P3DDT gel in 84.7% dodecane/15.3% DCB at isothermal conditions (30 °C).

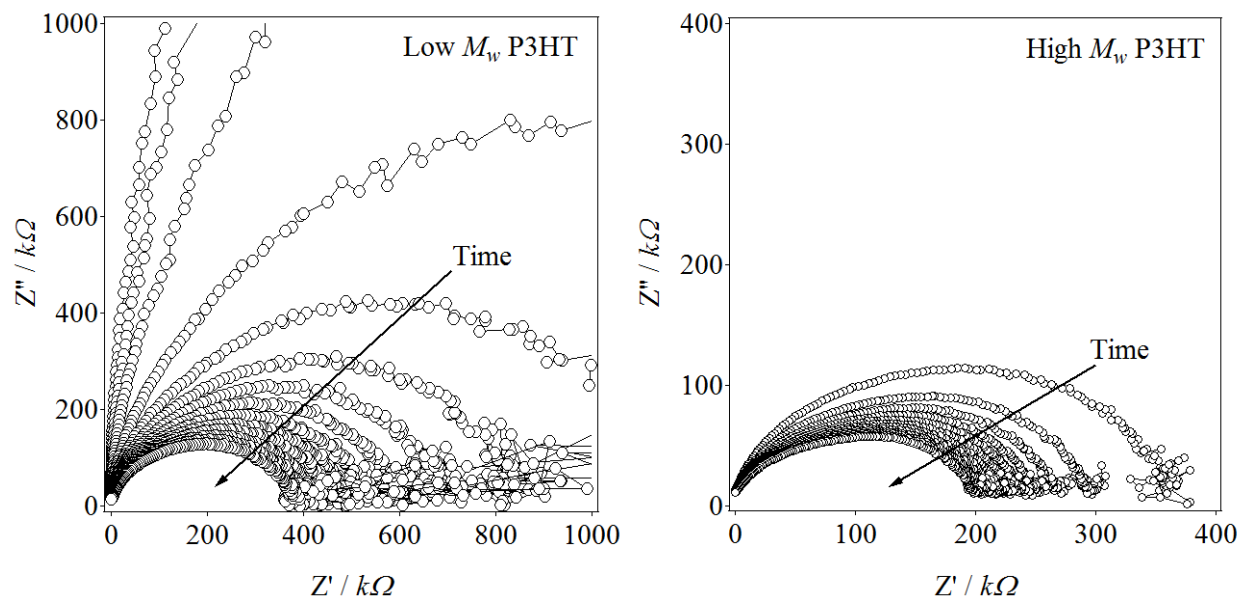


**Figure S7.** Nyquist plots for the self-assembly of a 30 mg/mL Low  $M_w$  P3HT gel in 27.5% dodecane/72.5% DCB at 20 °C (left) and of a 30 mg/mL High  $M_w$  P3HT gel in 43.9% dodecane/56.1% DCB at 30 °C (right).

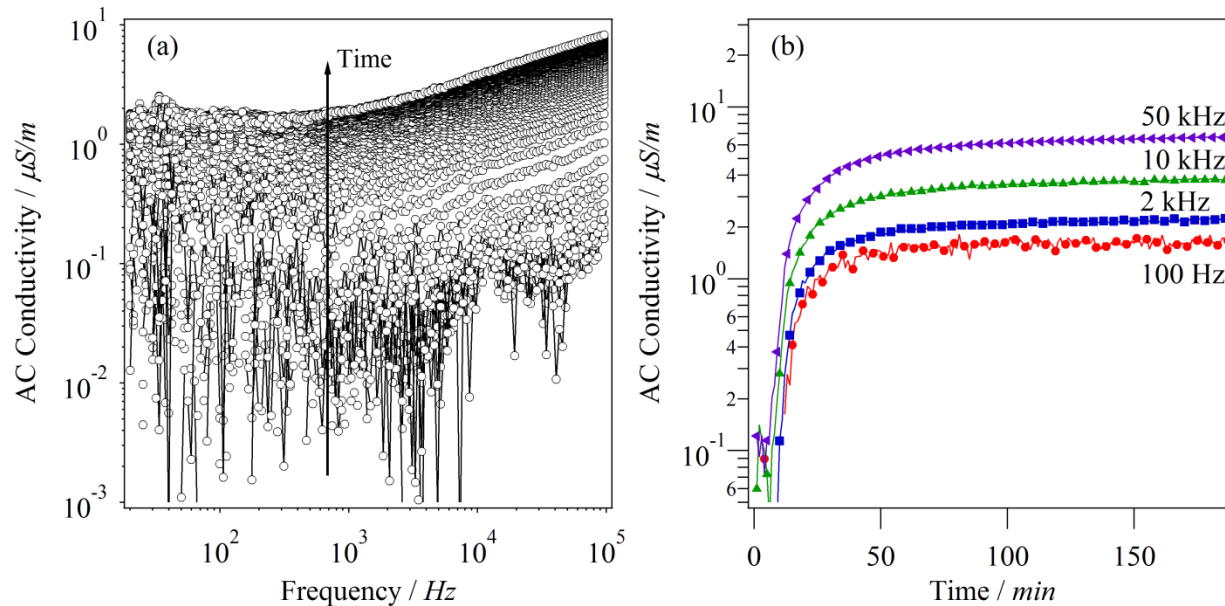


**Figure S8.** a) The AC conductivity as function of frequency taken during the self-assembly of a 30 mg/mL P3OT gel in 71.3% dodecane/28.7% DCB at isothermal conditions (30 °C). b) The AC conductivity plotted for multiple frequencies as a function of time at the same sample and self-assembly conditions.

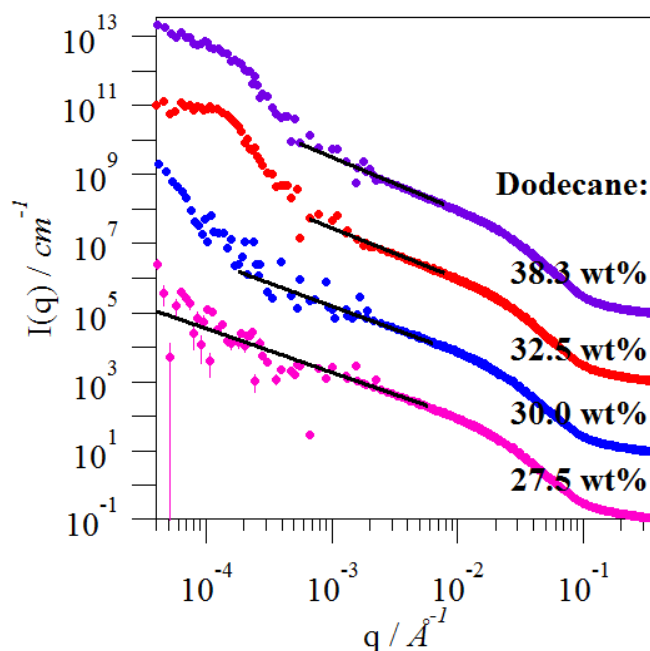


**Figure S9.** Combined SANS and desmeared USANS profiles, shifted for clarity, of 30 mg/mL low  $M_w$  P3HT in dodecane/1,2-dichlorobenzene solvent mixtures self-assembled for at least 24 hours at 20 °C. The network fractal dimension ( $D_f^S$ ) is extracted using a power law fit of the combined profiles and is shown as a black line. Power law exponents obtained by fitting the full range are within 5% of those obtained from fits constrained to the low- $q$  region of the SANS data.

### References:

1. P. Mittelbach and G. Porod, *Acta Physica Austriaca*, 1961, **14**, 185-211.
2. G. Newbloom, F. Kim, S. Jenekhe and D. Pozzo, *Macromolecules*, 2011, **44**, 3801-3809.
3. B. Hammouda, *Advances in Polymer Science*, 1993, **106**, 87-133.

4. G. M. Newbloom, K. M. Weigandt and D. C. Pozzo, *Macromolecules*, 2012, **45**, 3452-3462.
5. G. M. Newbloom, K. M. Weigandt and D. C. Pozzo, *Soft Matter*, 2012, **8**, 8854-8864.
6. K. S. Schweizer, *The Journal of Chemical Physics*, 1986, **85**, 1156-1175.
7. J.-L. M. Abboud and R. Notario, *Pure and Applied Chemistry*, 1999, **71**, 645-718.
8. P. de la Iglesia and D. C. Pozzo, *Soft Matter*, 2013, **9**, 11214-11224.
9. J. J. Richards, K. M. Weigandt and D. C. Pozzo, *Journal of Colloid and Interface Science*, 2011, **364**, 341-350.
10. L.-J. Zuo, X.-L. Hu, T. Ye, T. R. Andersen, H.-Y. Li, M.-M. Shi, M. Xu, J. Ling, Q. Zheng, J.-T. Xu, E. Bundgaard, F. C. Krebs and H.-Z. Chen, *The Journal of Physical Chemistry C*, 2012, **116**, 16893-16900.
11. N. Dingenouts, J. Bolze, D. Pötschke and M. Ballauff, in *Polymer Latexes - Epoxide Resins - Polyampholytes*, Springer Berlin Heidelberg, 1999, vol. 144, ch. 1, pp. 1-47.
12. J. W. Kiel, A. P. R. Eberle and M. E. Mackay, *Physical Review Letters*, 2010, **105**, 168701-168704.
13. J. W. Kiel, B. J. Kirby, C. F. Majkrzak, B. B. Maranville and M. E. Mackay, *Soft Matter*, 2010, **6**, 641-646.